



# Fast statistical model-based classification of epileptic EEG signals

Antonio Quintero Rincon, Marcelo Alejandro Pereyra, Carlos d’Giano,  
Marcelo Risk, Hadj Batatia

## ► To cite this version:

Antonio Quintero Rincon, Marcelo Alejandro Pereyra, Carlos d’Giano, Marcelo Risk, Hadj Batatia. Fast statistical model-based classification of epileptic EEG signals. *Biocybernetics and Biomedical Engineering*, 2018, 38 (4), pp.877-889. hal-01942293

**HAL Id: hal-01942293**

**<https://hal.science/hal-01942293>**

Submitted on 3 Dec 2018

**HAL** is a multi-disciplinary open access archive for the deposit and dissemination of scientific research documents, whether they are published or not. The documents may come from teaching and research institutions in France or abroad, or from public or private research centers.

L’archive ouverte pluridisciplinaire **HAL**, est destinée au dépôt et à la diffusion de documents scientifiques de niveau recherche, publiés ou non, émanant des établissements d’enseignement et de recherche français ou étrangers, des laboratoires publics ou privés.




## Open Archive Toulouse Archive Ouverte (OATAO)

OATAO is an open access repository that collects the work of Toulouse researchers and makes it freely available over the web where possible

This is an author's version published in: <http://oatao.univ-toulouse.fr/21264>

**Official URL:** <https://doi.org/10.1016/j.bbe.2018.08.002>

### **To cite this version:**

[Quintero Rincon, Antonio and Pereyra, Marcelo Alejandro and D'Giano, Carlos and Risk, Marcelo and Batatia, Hadj  *Fast statistical model-based classification of epileptic EEG signals*. (2018) Biocybernetics and Biomedical Engineering, 38 (4). 877-889. ISSN 0208-5216

Any correspondence concerning this service should be sent to the repository administrator: [tech-oatao@listes-diff.inp-toulouse.fr](mailto:tech-oatao@listes-diff.inp-toulouse.fr)

# Fast statistical model-based classification of epileptic EEG signals

Antonio Quintero-Rincón<sup>a,\*</sup>, Marcelo Pereyra<sup>b</sup>, Carlos D'Giano<sup>c</sup>,  
Marcelo Risk<sup>a,d</sup>, Hadj Batatia<sup>e</sup>

<sup>a</sup> Department of Bioengineering, Instituto Tecnológico de Buenos Aires (ITBA), Buenos Aires, Argentina

<sup>b</sup> School of Mathematical and Computer Sciences, Heriot-Watt University, Edinburgh, UK

<sup>c</sup> Centro Integral de Epilepsia y Telemetría, Fundación Lucha contra las Enfermedades Neurológicas Infantiles (FLENI), Buenos Aires, Argentina

<sup>d</sup> Consejo Nacional de Investigaciones Científicas y Técnicas (CONICET), Buenos Aires, Argentina

<sup>e</sup> University of Toulouse, IRIT – INPT, Toulouse, France

## ARTICLE INFO

### Keywords:

Generalized Gaussian distribution

Wavelet filter banks

EEG

Epilepsy

Leave-one-out cross-validation

Linear classifier

## ABSTRACT

This paper presents a supervised classification method to accurately detect epileptic brain activity in real-time from electroencephalography (EEG) data. The proposed method has three main strengths: it has low computational cost, making it suitable for real-time implementation in EEG devices; it performs detection separately for each brain rhythm or EEG spectral band, following the current medical practices; and it can be trained with small datasets, which is key in clinical problems where there is limited annotated data available. This is in sharp contrast with modern approaches based on machine learning techniques, which achieve very high sensitivity and specificity but require large training sets with expert annotations that may not be available. The proposed method proceeds by first separating EEG signals into their five brain rhythms by using a wavelet filter bank. Each brain rhythm signal is then mapped to a low-dimensional manifold by using a generalized Gaussian statistical model; this dimensionality reduction step is computationally straightforward and greatly improves supervised classification performance in problems with little training data available. Finally, this is followed by parallel linear classifications on the statistical manifold to detect if the signals exhibit healthy or abnormal brain activity in each spectral band. The good performance of the proposed method is demonstrated with an application to paediatric neurology using 39 EEG recordings from the Children's Hospital Boston database, where it achieves an average sensitivity of 98%, specificity of 88%, and detection latency of 4 s, performing similarly to the best approaches from the literature.

\* Corresponding author at: Department of Bioengineering, Instituto Tecnológico de Buenos Aires (ITBA), Av. Eduardo Madero 399, C1106ACD Buenos Aires, Argentina.

E-mail address: [aquinter@itba.edu.ar](mailto:aquinter@itba.edu.ar) (A. Quintero-Rincón).  
<https://doi.org/10.1016/j.bbe.2018.08.002>

## 1. Introduction

Epilepsy is a disease that produces brain activity disorders [1–3]. Its diagnosis relies strongly on the analysis of electroencephalography (EEG) data, a non-invasive and widely available biomedical modality that allows neurologists to monitor abnormal activity and characterize its nature. In particular, neurologists analyze characteristic waveforms to localize and quantify the epileptogenic zone. These brain activity disorders can lead to epileptic seizures that have a sudden onset, spread quickly, and are very brief.

Epileptic seizure detection methods based on EEG signals stem from the observation that EEG signal descriptors allow discriminating between normal and abnormal brain activity. This practice originated half a century ago with works by Viglione et al. [4], Liss et al. [5], Ktonas et al. [6] and Gotman et al. [7]; and continued with Iasemidis et al. [8,9] mainly in the medical literature and by using analogue EEG devices. Later, as EEG systems adopted digital signal processing capacity, this stimulated the development of pattern recognition methods to detect and analyse abnormal brain activity automatically. A main practical advantage of EEG technology is that it is very economically accessible. This has significantly contributed to the wide adoption of EEG in developing countries (whereas other more advanced modalities, such as magnetoencephalography (MEG), are expensive and have not been widely adopted as a result).

There are currently a wide range of EEG signal processing methods to detect brain seizures accurately. Most methods use classification techniques from the supervised machine learning literature, such as support vector machines [10–12] and discriminant analysis [13], and differ mainly in terms of their feature extraction methods and the features classification approaches. Many methods use time-frequency descriptors, either explicitly (e.g., short-term Fourier or wavelet representations) [14–17,11,18,19], empirical mode decomposition [20–22], or implicitly by learning neural networks [23–25] or by using component analysis or common spatial patterns (see for example [26–28]). Some also use statistical descriptors such as signal entropy [17,11,29–31] or fractal dimension [32,33].

The main approaches from the state of the art are summarised in Table 1, together with their detection performance on a test dataset. Observe that most modern methods perform remarkably well and achieve true positive rates (TPR) or sensitivities of the order of 95–99%, and true negative rates or specificities of the order of 85–95%, depending on the specific method and dataset considered. This good performance is achieved by using advanced signal processing techniques that are generally very computationally intensive. As a result, state-of-the-art detection methods cannot be incorporated into EEG devices to perform detection in real time. For example, the method [26] uses common spatial patterns that require estimating covariance matrices and performing singular value decompositions at each detection step. This limitation is motivating the development of detection methods that use cloud computing technology to perform detection on a high performance computing server that is accessed remotely (see for example [28]). This strategy is potentially very interesting in some settings, but it would be

difficult to implement in developing countries where many hospitals still have limited Internet access and poor IT infrastructure.

Another limitation of state-of-the-art methods is that they pull information from all spectral bands to improve detection performance [26]. While beneficial in terms of classification accuracy, this can be problematic in many clinical applications where the current practice is to detect seizures independently in each physiological spectral band or *brain rhythm* (these bands are specified in Section 2). Finally, state-of-the-art methods also rely increasingly on large training datasets, which is a drawback in clinical applications where there is limited annotated data available. Also, many existing methods use feature-based classification techniques, with a significant number of features in order to handle the inherent variability of such features.

This paper seeks to address these limitations of the existing methodology by developing an automatic EEG detection technique that has low computational cost, that performs detection independently in each brain rhythm following current clinical practice, and that can be trained with small datasets, with a detection performance that is similar to that of state-of-the-art algorithms. In contrast with existing methods, the proposed method adopts a model-based classification approach. Model-based classification has been used in various applications [34–36]. The idea is to capture the statistical properties of the signal using the parameters of a probabilistic model. This approach is interesting compared to feature-based classification, especially when features are numerous or exhibit large variability. It can be viewed as an interesting dimensionality reduction technique facing the curse of dimensionality and leading to low computational cost classification. Despite its interest, this approach has not been widely investigated in EEG signal processing. Precisely, our classification method is driven by a parametric statistical model that captures the statistical properties of the signals and their evolution in time, with the model parameters acting as classification features. This approach is an interesting alternative to the non-parametric features (e.g., signal power spectrum, variance, entropy, etc.) commonly used in the literature because the parametric structure of the model acts as a dimensionality reduction mechanism that regularizes the classification problem and consequently improves the stability and robustness of the classification, and which at the same time significantly reduces the associated computational cost. Despite its advantages, to the best of our knowledge this promising approach has not been investigated for EEG signal classification. Note however that statistical approaches have been successfully applied to other challenging EEG processing problems (see for example [37,38]).

The remainder of the paper is structured as follows. Section 2 introduces notation and specifies the detection problem considered. Section 3 presents the proposed method, with its three main steps detailed in Sections 3.1–3.3. Section 4 presents a range of experimental results with EEG recordings from the Children's Hospital Boston database and reports detection performance in terms of sensitivity, specificity, and latency. Advantages and limitations, Conclusions and perspectives for future work are finally reported in Sections 5 and 6 respectively.

**Table 1 – State-of-the-art methods to perform seizure detection automatically in EEG signals, summarised in terms of the classification techniques and features used and their reported performance on a test dataset. The performance metrics are the True Positives Rate or Sensitivity (TPR), the True Negative Rate or Specificity (TNR) and the Accuracy (ACC).**

Classification method	Features	Test data	Performance	Ref.
Learning vector quantization	Signal entropy from wavelet coefficients	400 epochs from 5 normal subjects and 5 epileptic patients	TPR:98%	[17]
Support Vector Machine	Matching pursuit algorithm	133 EEG from Rigshospitalet University Hospital database (Copenhagen, Denmark)	TPR:78%, TNR:84%	[10]
Support Vector Machine	Spectral and Entropy Analysis	3 datasets from EEG University Hospital Bonn database	TPR:90%	[11]
Fuzzy classification	Amplitude, frequency and entropy descriptors	56 iEEG from 20 patients from University of Freiburg database	TPR:95.8%, TNR:74%	[18]
Hidden Markov Model	Segmentation of topographic maps of time varying spectral	10 EEG patients from EPILEPSIAE [39]	TPR:94.59%, TNR:92.22%	[19]
Support Vector Machine	Third-order tensor discriminant analysis: spectral, spatial, and temporal domains	36 EEG patients from Children's Hospital Boston database	TPR:98%, TNR:94%	[13]
K-means clustering	Spatiotemporal Analysis as morphological filter	10 EEG patients from University of Florida Hospital database	TPR:87.4%	[40]
Logistic classifier	Stacked autoencoders neural network	36 EEG patients from Children's Hospital Boston database	TPR:100%	[23]
Support Vector Machine	Fractional linear prediction	100 single channel EEG segments from The Bern-Barcelona EEG database	TPR:96%, TNR:95%	[41]
Least Squares Support Vector Machine	Phase space representation	100 segments from the EEG University Hospital Bonn	TPR:100%, TNR:96%	[42]
Support Vector Machine	Empirical mode decomposition	51 EEG segments from 17 patients from University of Freiburg (Germany)	TPR:98.6%, TNR:88.6%	[43]
1-Nearest Neighbor	1D-local binary patterns from bank of Gabor filters	100 ECoG segments from University Hospital Bonn database	TPR:98.33%	[44]
Support Vector Machine	Common Spatial Pattern	36 EEG patients from Children's Hospital Boston database	TPR:100%	[26]
Relevance Vector Machine	Multifractal formalism	21 EEG patients from the Epilepsy Center of the University Hospital of Freiburg	TPR:92.94%, TNR:97.47%	[45]
Regression neural network	Statistical descriptors of dual-tree complex wavelet transform coefficients	100 segments from University of Bonn database and 21 patients from Sir Ganga Ram Hospital (New Delhi)	TPR:92%, TNR:98%	[24]
K-Nearest Neighbor, linear discriminant analysis, naive Bayesian, logistic regression and Support Vector Machine	Time, frequency, time-frequency and nonlinear features	100 segments from University Hospital Bonn database	TPR:99.25%	[46]
1-Nearest Neighbor	Convolutional neural network	5 patients from the EEG University Hospital Bonn	TPR:95%, TNR:88.67%	[27]
Random Forest, C4.5, Functional tree, Bayesian-network, Naive-Bayes and K-nearest neighbours	Mean of joint instantaneous amplitude, Mean monotonic absolute change and Variance of monotonic absolute change from Empirical wavelet transform	36 EEG patients from Children's Hospital Boston database	TPR:97.91%, TNR:99.57%	[47]
Multilayer perceptron neural network	Time-frequency localized three-band synthesis wavelet filter bank and subband norm	100 segments from University Hospital Bonn database	ACC: 99.66%	[48]
Support Vector Machine	Pyramid of difference of Gaussian filtered signals and Local binary patterns	100 segments from the EEG University Hospital Bonn	TPR:100%, TNR:100%	[49]
Support Vector Machine	Random subspace ensemble method and Infinite Independent Component Analysis	208 ECoG from University of Pennsylvania and the Mayo Clinic	TPR:98%, TNR:96%	[28]
Least-Square Support Vector Machine	Time-frequency representation based on the improved eigenvalue decomposition of Hankel matrix and Hilbert transform	100 segments from the EEG University Hospital Bonn	TPR:100%, TNR:100%	[50]

## 2. Problem statement

Let  $\mathbf{X} \in \mathbb{R}^{M \times N}$  denote a time-discretized EEG signal recorded by an array composed of  $M$  channels over a period of  $T$  seconds, and using a sampling period of  $T/N$  seconds. Each row of  $\mathbf{X}$  is associated with one channel of the array and contains all the sampling points corresponding to the EEG signal recorded by that channel, whereas each column is associated with a sampling point and contains the vector signal acquired by the full array at that time instant. Moreover, to analyse the different frequency components of  $\mathbf{X}$ , we denote by  $\mathbf{X}_\delta$ ,  $\mathbf{X}_\theta$ ,  $\mathbf{X}_\alpha$ ,  $\mathbf{X}_\beta$ , and  $\mathbf{X}_\gamma$  the spectral components related to the  $\delta$  (0–4 Hz),  $\theta$  (4–8 Hz),  $\alpha$  (8–16 Hz),  $\beta$  (16–32 Hz), and  $\gamma$  (32–64 Hz) frequency bands. As mentioned previously, each of these bands is related to different neurological functions and is therefore associated with specific neurological disorders.

This paper considers the problem of detecting epileptic seizure activity in EEG signals in real-time, and identifying the frequency bands where the seizure occurs. Formally, for any time instant  $n \in \{1, N\}$ , define band-specific binary labels  $z_\delta(n)$ ,  $z_\theta(n)$ ,  $z_\alpha(n)$ ,  $z_\beta(n)$ , and  $z_\gamma(n)$  that take value 1 to indicate the presence of an epileptic seizure at their spectral band, and 0 to indicate normal activity. Given some expert annotated training data  $\{\mathbf{X}_0^{(k)}\}_{k=1}^{K_0}$  and  $\{\mathbf{X}_1^{(k)}\}_{k=1}^{K_1}$  corresponding to short EEG recordings of healthy and epileptic seizure activity, we consider the supervised classification problem of estimating the values of  $z_\delta(n)$ ,  $z_\theta(n)$ ,  $z_\alpha(n)$ ,  $z_\beta(n)$ , and  $z_\gamma(n)$  in real-time as  $\mathbf{X}$  is acquired by the EEG array. Similarly to [14], because we are interested in clinical applications where this information is required in real-time, we focus on classifiers that have low computational complexity.

## 3. Proposed method

This section presents a new method to detect epileptic seizures in EEG signals and simultaneously identify the frequency bands where the seizure occurs. As mentioned previously, the main strengths of the methodology are that it can be trained with small training datasets, and that it is computationally very efficient and suitable for performing detection in real-time.

The proposed method has a pipeline structure composed of the following three steps: a filter bank that separates  $\mathbf{X}$  into its  $\mathbf{X}_\delta$ ,  $\mathbf{X}_\theta$ ,  $\mathbf{X}_\alpha$ ,  $\mathbf{X}_\beta$ , and  $\mathbf{X}_\gamma$  spectral components, followed by a statistical dimensionality reduction step that maps these components into a low-dimensional representation where pathological brain activity is easily detected, and finally a classification step based on a thresholding approach. This structure is summarised in the diagram in Fig. 1.

### 3.1. Spectral decomposition by wavelet filter bank

We use a Daubechies (Db4) wavelet filter bank to separate  $\mathbf{X}$  into the five spectral components  $\mathbf{X}_\delta$ ,  $\mathbf{X}_\theta$ ,  $\mathbf{X}_\alpha$ ,  $\mathbf{X}_\beta$ , and  $\mathbf{X}_\gamma$  [51] (we use Db4 because it offers the number of vanishing moments that allow representing the signal with sufficient smoothness). Performing wavelet decomposition fits naturally the dyadic structure of the neurological spectral bands, and provides a computationally efficient filtering algorithm that can be

implemented straightforwardly on real-time signal processing hardware. Because our data is acquired at a 256 Hz sampling rate, in our experiments we use a wavelet filter through tree-based topology, with six scales. The upper five scales match with the spectral bands of interest (the remaining scale related to the 64–128 Hz band has very poor signal-to-noise ratio and is discarded). The output of this stage are 5 sets of wavelet coefficients  $\Omega_\delta$ ,  $\Omega_\theta$ ,  $\Omega_\alpha$ ,  $\Omega_\beta$ ,  $\Omega_\gamma$  (observe that this approach can be straightforwardly generalized to higher sampling rates by using or discarding any additional bands).

### 3.2. Statistical model of the spectral components

Designing a classifier to detect pathological brain activity directly from the EEG signals (or their wavelet representation) is very challenging due to the high-dimensionality of the data, and because it would require a large training set and a complex classification methodology. To detect abnormal brain activity with limited annotated training data, particularly in the context of classifiers with low computational complexity suitable for real-time implementations, it is necessary to map the EEG data to a meaningful compact representation that highlights the information able to discriminate normal and abnormal activities. A successful representation should also provide the low-dimensional structure and favorable regularity properties that enable a simple classification scheme, such as threshold-based methods.

Here we construct this representation by using a parametric statistical model to summarize the empirical distribution of the wavelet coefficients associated with each spectral band. Precisely, we adopt a sliding window approach and fit a parametric statistical model to the wavelet coefficients associated with the last 2 s of  $\mathbf{X}$ . Because the signals we consider in our experiments are acquired with  $M = 23$  channel array, the 2-s window corresponds respectively to the last 8192, 4096, 1024, 512 and 256 coefficients of  $\Omega_\delta$ ,  $\Omega_\theta$ ,  $\Omega_\alpha$ ,  $\Omega_\beta$ , and  $\Omega_\gamma$ . We model each set of wavelet coefficients with zero-mean generalized Gaussian distribution (GGD) with density given by

$$f(s; \sigma, \tau) = \frac{\tau}{2\sigma\Gamma(\tau-1)} \exp\left(-\left|\frac{s}{\sigma}\right|^\tau\right) \quad (1)$$

where  $\sigma \in \mathbb{R}^+$  is a scale parameter,  $\tau \in \mathbb{R}^+$  is a shape parameter that controls the density tail, and  $\Gamma(\cdot)$  is the Gamma function (we estimate the values of  $\sigma$  and  $\tau$  for each spectral band by maximum likelihood estimation, which we solve straightforwardly by using a Newton–Raphson algorithm [52]). Therefore, at a given time point  $n$ , the  $\sum_{j=9}^{13} 2^j = 15872$  wavelet coefficients corresponding to the 2-s window are mapped to a 10-dimensional representation  $\sigma(n) = [\sigma_\delta(n), \sigma_\theta(n), \sigma_\alpha(n), \sigma_\beta(n), \sigma_\gamma(n)]$ ,  $\tau(n) = [\tau_\delta(n), \tau_\theta(n), \tau_\alpha(n), \tau_\beta(n), \tau_\gamma(n)]$ . In addition to bringing significant dimensionality reduction, the experiments reported in Section 4 show that this approach maps each neurological spectral band onto a two-dimensional representation where seizures are easily discriminated and can be detected accurately with a linear classifier. From a EEG physics viewpoint, the parameters  $\sigma(n)$  and  $\tau(n)$  capture the statistical distribution of the power of the EEG signal array at time  $n$  in each spectral band;  $\sigma(n)$  measures the average power in each band, and  $\tau(n)$  the deviations of power from these average values [53].

As mentioned previously, parametric approaches are regularized by their parametric structure and as a result they

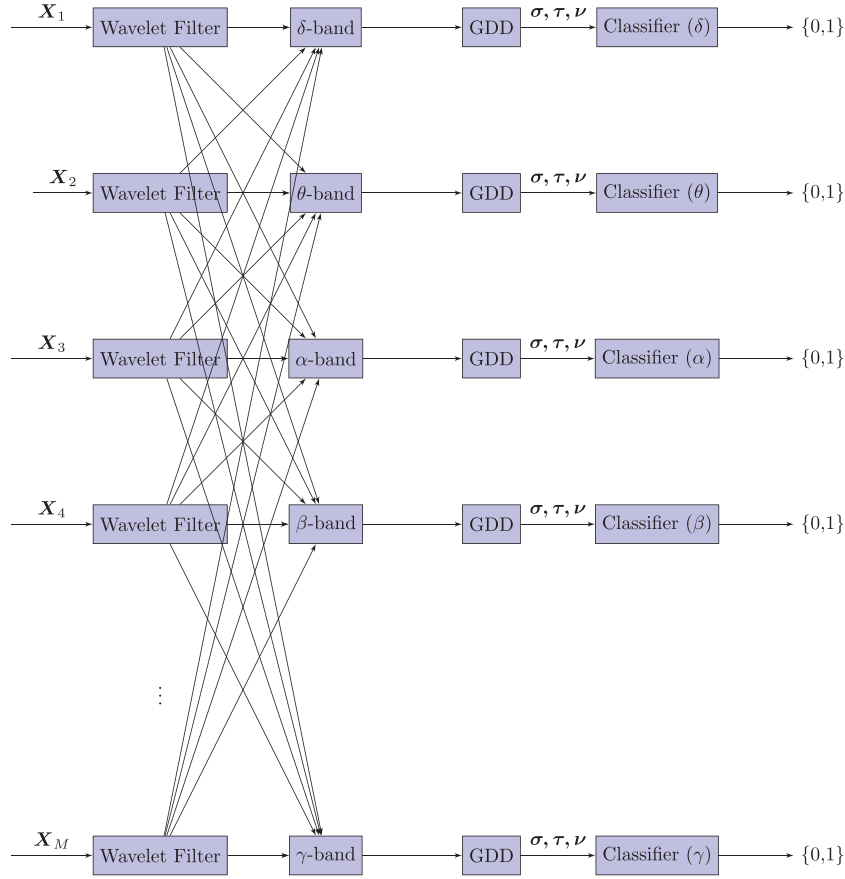


**Fig. 1 – Block-diagram representation of the proposed method to detect epileptic seizures in EEG signals. The method consists of three main steps: separation of brain rhythms using wavelet-bank filtering, statistical model-based dimensionality reduction using a generalized Gaussian distribution (GGD), and seizure detection using classification through linear discriminant analysis.**

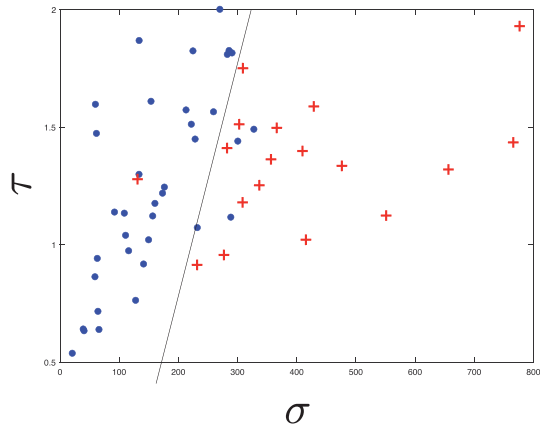
achieve good performance results with smaller datasets compared to non-parametric approaches. However, non-parametric strategies tend to be superior when a large amount of training data is available because they are more flexible and consequently can better exploit the information provided by the data (whereas parametric models are constrained by their structure and hence suffer from intrinsic estimation bias due to model misspecification). Similarly, over-parameterised strategies, e.g., machine learning techniques based on neural networks, also perform very well in data rich settings.

Finally, it is mentioning that we also considered other statistical models for the wavelet coefficients, namely the logistic, t-location scale, and symmetric  $\alpha$ -stable distributions. We found that the generalized Gaussian model provided the best model-fit-to-data (we conducted these comparisons using real data from the Children's Hospital Boston database [54,14] – see results in [Appendix A](#)).

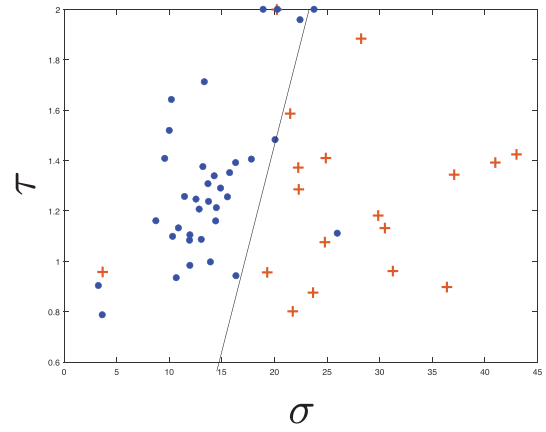
### 3.3. Seizure detection by linear discriminant analysis classification

The final stage of the proposed seizure detection pipeline is a classifier that labels the statistical parameters associated

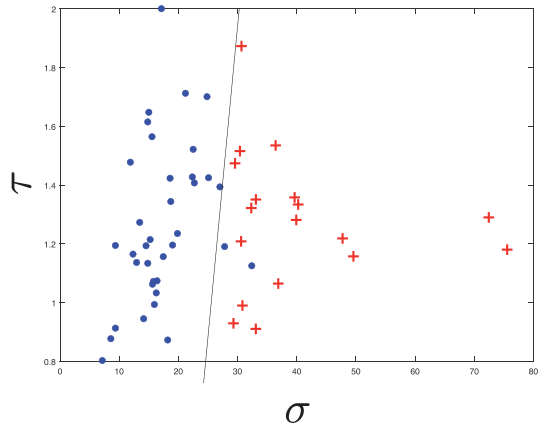
with each spectral band as *seizure* or *non-seizure*. Precisely, five independent two-parameter classifiers are used in parallel to classify the pairs  $[\sigma_\delta(n), \tau_\delta(n)]$ ,  $[\sigma_\theta(n), \tau_\theta(n)]$ ,  $[\sigma_\alpha(n), \tau_\alpha(n)]$ ,  $[\sigma_\beta(n), \tau_\beta(n)]$ , and  $[\sigma_\gamma(n), \tau_\gamma(n)]$  generated by the statistical dimensionality reduction step. This allows to simultaneously identify seizure activity and the spectral bands where it occurs. For simplicity we use linear classifiers derived from a linear discriminant analysis. Precisely, we adopt a supervised approach where each classifier is band-specific and has been trained by performing a linear discriminant analysis on expert annotated data. We perform the discriminant analysis on an augmented vector  $[\sigma, \tau, \nu] \in \mathbb{R}^3$ , where  $\nu = \sigma^2 \Gamma(3/\tau) / \Gamma(1/\tau)$  is a variance parameter. Including  $\nu$  in the discriminant analysis embeds  $(\sigma, \tau)$  in a non-linear manifold in  $\mathbb{R}^3$  where a better linear classification is possible (note that  $\nu$  is available for free as a by-product of the Newton-Raphson method that estimates  $\sigma$  and  $\tau$ , hence this augmentation does not introduce any additional computational cost). The resulting linear classifiers are specified by three parameters  $(a, b, c)$  defining a plane that splits  $\mathbb{R}^3$  in two regions related to *seizure* and *non-seizure* events, and which essentially operate as a three-dimensional threshold for the triplets  $\sigma, \tau, \nu$ . Lastly, similarly to the choice of the statistical model, it is possible to consider more advanced



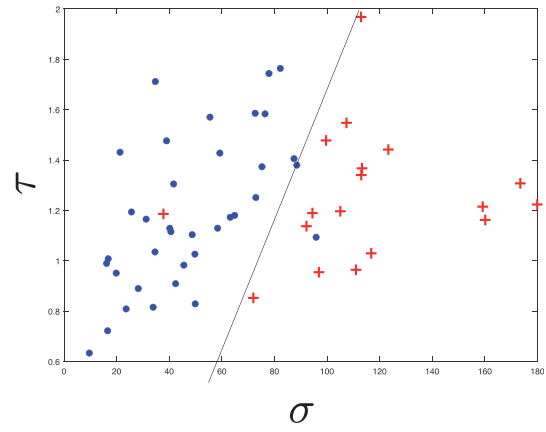
(a) Delta Band



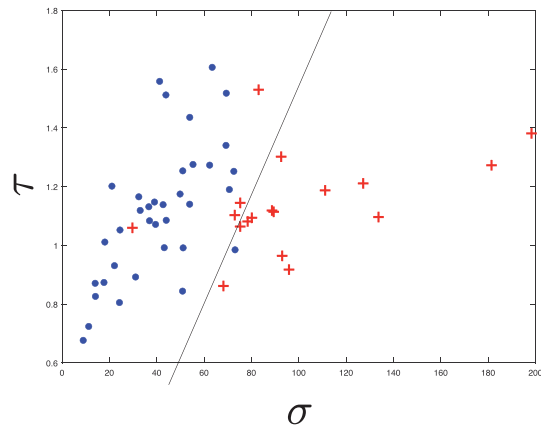
(b) Theta Band



(c) Alpha Band



(d) Beta Band



(e) Gamma Band

**Fig. 2 – Scatter plots for the statistical parameters  $\sigma$  and  $\tau$  for seizure signals (red cross) and non-seizure signals (blue circles) for each spectral band, showing the good discrimination properties of the proposed representation.**

classifications schemes. However, such classifiers also involve more parameters and hence are more prone to over-fitting and more computationally expensive.

#### 4. Experimental results

We now demonstrate the proposed methodology with experiments with real data and comparisons with other approaches from the literature. For the experiments we used data from the Children's Hospital Boston database [54], previously considered in [14], which consists of 36 EEG recordings from pediatric subjects with challenging seizures. (The signals were acquired with a 23-channel array operating at a 256 Hz sampling rate). From this database, we used 13 seizure signals or *epochs* selected by an experienced neurologist, see Table 4. These correspond to 13 seizure events from 9 different subjects, and are between 1 and 5 min long (the other data exhibited strong artifacts related to muscle activity and were discarded as a consequence). The neurologist annotated each signal to indicate the beginning and ending of the seizure epochs, which we use as ground truth. Moreover, for each seizure epoch, the neurologist also selected two adjacent non-seizure signal segments of the same length to represent challenging non-pathological brain activity. The resulting dataset consisted therefore of 39 signal segments related to 13 seizures and 26 non-seizure signals, and of variable length in the range of 1–5 min.

To illustrate the capacity of the statistical parameters  $\sigma$  and  $\tau$  to discriminate seizure events and non-seizure signals, Fig. 2 shows scatter plots for each spectral band constructed using the signals in the database and the expert annotations (non-seizure signals are represented using blue circles and seizure signals using red crosses). Observe that this representation provides a very good linear discrimination of the seizure and non-seizure groups. In particular, one notices that the scale parameter  $\sigma$  is particularly useful for discrimination (see also discrimination tests in Appendix B).

Moreover, to assess the performance of the proposed methodology, we adopted a supervised testing approach

and used the 39 signal segments described above to train and test the method. Because the dataset is relatively small we used an exhaustive cross-validation technique based on a leave-one-out approach. Precisely, at each iteration of the cross-validation process we trained the 5 classifiers (each defined by 3 parameters) with data from 13 seizure signals and 26 non-seizure signals, and then assessed classification performance on the remaining 3 signals (these are 1 seizure and 2 non-seizure signals). In each iteration of the cross-validation process the classification performance was assessed by splitting the test signals into sequences of 2 s and classifying each sequence individually; these results were then used to assess classification performance. Precisely, we measure the method's true positive rate (TPR) or *sensitivity*, false positive rate (FPR), true negative rate (TNR) or *specificity*, and overall accuracy (ACC), expressed as the percentage of good classification. For each figure of merit we report the mean value and the standard deviation. These results are reported in Table 2. We also report latency (time delay) between the annotated seizure onset and the detection by the method in Table 3. We compare classification accuracy and latency with the state-of-the-art methods [13,26,23], which also report classification performance and latency for the Children's Hospital Boston database. We emphasise again that these state-of-the-art methods are significantly more computationally expensive than the proposed method. For example, [13] uses a third-order tensor discriminant analysis, [23] a stack of neural networks combined with a logistic classifier, and [26] computes singular value decompositions of covariance matrices at each detection step. Neither of these methods can be implemented in real-time in a standard EEG system as a consequence.

Observe from Table 2 that, despite the computational simplicity, the proposed method achieves an excellent sensitivity of the order of 97–99% for all spectral bands on the test dataset. This is close to the state-of-the-art performances of 98–100% reported in [13,26,23] for this dataset. Moreover, the specificity of the proposed method is approximately 90%. This is slightly below the 94% specificity of [13] (the works [26,23] do not report specificity). However, notice

**Table 2 – Seizure detection performance for each brain rhythm and for 39 events (13 seizure and 26 non-seizure) of the Children's Hospital Boston database, in terms of: TPR = True Positives Rate or Sensitivity; TNR = True Negative Rate or Specificity; FPR = False positive Rate; and ACC = Accuracy [average value  $\pm$  standard deviation].**

Metric	Delta Band ( $\delta$ )	Theta Band ( $\theta$ )	Alpha Band ( $\alpha$ )	Beta Band ( $\beta$ )	Gamma Band ( $\gamma$ )
TPR	0.97 $\pm$ 0.06	0.99 $\pm$ 0.01	0.99 $\pm$ 0.02	0.97 $\pm$ 0.05	0.99 $\pm$ 0.01
TNR	0.92 $\pm$ 0.07	0.79 $\pm$ 0.23	0.91 $\pm$ 0.08	0.90 $\pm$ 0.10	0.91 $\pm$ 0.08
FPR	0.08 $\pm$ 0.07	0.21 $\pm$ 0.23	0.09 $\pm$ 0.08	0.10 $\pm$ 0.10	0.09 $\pm$ 0.08
ACC	95.13 $\pm$ 4.64	92.69 $\pm$ 7.61	96.59 $\pm$ 2.99	94.48 $\pm$ 5.77	97.00 $\pm$ 2.88

**Table 3 – Average latency between seizure onset and detection (in seconds), for the proposed method on each spectral band, and for the state-of-the-art methods [13,26,23].**

Proposed					State-of-the-art		
Delta band ( $\delta$ )	Theta band ( $\theta$ )	Alpha band ( $\alpha$ )	Beta band ( $\beta$ )	Gamma band ( $\gamma$ )	[13]	[26]	[23]
4.3	3.9	4.1	4.0	4.1	4.5	3.4	7.2

**Table 4 – Length of the 18 Seizures used in this study and the corresponding number of 2-s segments. An offset has been used for each epoch to avoid leading and trailing signals that were noisy. Consequently, the number of windows is irregular between epochs.**

Epoch	Seizure	Duration	Segments	Processing duration in ms				
				Delta	Theta	Alpha	Beta	Gamma
01	04	1m30sec	181	7	6	7	7	8
02	05	1m41sec	203	7	7	7	8	9
03	10	1m04sec	129	7	7	7	7	9
04	11	1m07sec	137	7	6	7	7	8
05	12	2m00sec	241	7	7	7	8	8
06	13	1m57sec	235	7	7	7	8	9
07	17	1m26sec	173	7	7	7	8	8
08	18	2m23sec	287	7	7	7	8	9
09	19	3m09sec	321	7	6	6	7	8
10	20	3m46sec	343	7	6	6	7	8
11	21	5m38sec	529	7	6	7	7	8
12	22	1m04sec	129	7	6	7	7	8
13	23	1m03sec	125	7	9	9	7	13
14	26	1m05sec	131	7	9	10	11	35
15	27	1m02sec	117	7	7	7	7	9
16	28	1m16sec	153	7	7	7	8	9
17	29	1m29sec	179	7	6	7	7	8
18	30	0m32sec	65	7	7	7	7	8

that to achieve this higher specificity, the method [13] pulls together all spectral bands, and as a result it does not discriminate between seizures in different bands. Our method performs classification independently on each band because this is useful in clinical practice, at the expense of a slightly a lower specificity.

Furthermore, observe from Table 3 that our method achieves an average latency of approximately 4 s for all spectral bands, outperforming the state-of-the-art methods [13,23] and close to the fastest available method [26]. We emphasise at this point that all the latency values reported in the literature measure the delay of the detection algorithm offline, without taking into account any overhead related to the methods' computing times. Therefore, the fact that different methods achieve similar latency does not indicate that they have similar computational complexity.

Note that we do not report computing times for these experiments for two reasons. First, because we have conducted these proof-of-concept tests in MATLAB, and processing each 2-s EEG signal window required less than 50 ms. Second, because we do not have access to the implementations of [13,26,23], and therefore the comparisons would not be fair. However, as explained previously, these methods clearly have a significantly higher computational complexity because of the sophisticated mathematical operations involved (e.g., third-order tensor discriminant analysis, singular value decompositions of covariance matrices, stacked neural networks, etc.). A real-time implementation of the proposed method is currently under development.

Finally, we emphase at this point that the sensitivity and specific values reported above are for the specific test dataset [54], which is limited in many ways. To reliably determine the sensitivity and specificity of the method in a clinical setting it is necessary to conduct a thorough evaluation by using long-term and continuous EEG signals (see for example the

protocols adopted in [55]). A thorough evaluation of the performance of the proposed methods is a main perspective for future work.

## 5. Advantages and limitations of the proposed method

Through the use of a statistical model-based classification technique, the proposed method has three main advantages. First, it requires only estimating and classifying two scalar parameters allowing it to be implemented in dedicated real time hardware. Second, it can be trained using a reasonably small dataset due precisely to the fact that it used only two classification parameters. This contrasts with methods using a number of features that would require large training datasets. Third, it allows seizure detection simultaneously in the different brain rhythms, complying with current medical practices.

Nevertheless, the proposed method has three main limitations. First, due to the very high dynamics of epileptic signals, defining the sliding time-window and the overlap of epochs is difficult. Second, it needs defining regularization parameters for the training stage in order to take into consideration random peaks, noise and artefacts that might lead to false positives. Third, seizures have variable and dynamic offsets corresponding to the complex nature of different epilepsy types. As an example, when brain waves slow down, change from seizure to *non-seizure* is difficult to track and can generate classification errors.

## 6. Conclusions

This paper presented a new classification method to detect epileptic brain activity in EEG signals, with a focus on

applications involving real-time constraints and small training datasets. An additional advantage of the method is that detection is performed independently for each brain rhythm, following the current medical practices. Detection is achieved by first separating the EEG signals into the five brain rhythms by using a wavelet decomposition, and then using a generalized Gaussian statistical model to map signals onto a low-dimensional representation where classification can be performed efficiently by linear discriminant analysis. Experiments with 39 signals from 9 patients of the Children's Hospital Boston database and comparisons with other approaches from the literature indicate that the method achieves a very good sensitivity and a good specificity. Future work will focus on a thorough evaluation of the proposed method in a pre-clinical setting, by using long-term and continuous EEG signals and the protocols presented in [55]. Another important perspective consists in studying spatial EEG source location information to characterize the spatio-temporal patterns of epileptic activity. A real-time implementation of the proposed method on an EEG monitoring system is currently under development.

## Acknowledgements

This work was supported by the SuSTaIN program, EPSRC grant EP/D063485/1 at the Department of Mathematics, University of Bristol; ITBACyT grant DP.557No.34/2015, Instituto Tecnológico de Buenos Aires; 07/15Protocol at FLENI; and the DynBrain project supported by the STICAmSUD international program. Part of the work was conducted when MP held

a Marie Curie Intra-European Fellowship for Career Development at the School of Mathematics of the University of Bristol. Also, part of the work has been presented at the IEEE IVMSP, IMFBE, and Journal of Physics conferences [56–58].

## Appendix A. Goodness-of-fit measures for the statistical models of the EEG wavelet coefficients $\Omega_\delta, \Omega_\theta, \Omega_\alpha, \Omega_\beta, \Omega_\gamma$

We assessed the goodness-of-fit of the generalized Gaussian model for the EEG wavelet coefficients  $\Omega_\delta, \Omega_\theta, \Omega_\alpha, \Omega_\beta, \Omega_\gamma$  by computing the Kolmogorov-Smirnov (KS) score [59] and the Cramer-von-Mises (CvM) score [60]. For comparison, we also computed the goodness-of-fit score for the following other two-parameter statistical models that are also commonly used to model wavelet coefficients: logistic, t-location scale, and alpha-stable distributions. Moreover, we computed the scores for each spectral band and by separating the data into seizure and non-seizure groups. The resulting scores are summarized in Tables 5 and 6, which report respectively the mean and the standard deviation of the KS and the CvM scores. Observe that the generalized Gaussian distribution clearly provides the best model-fit-to-data.

## Appendix B. Model based characterization

In order to use the parameters  $\sigma$  and  $\tau$  as features to classify seizure and non-seizure EEG segments, we first propose to assess

**Table 5 – Means of the KS and CvM scores obtained for GGD pdfs estimated with all EEG segments of the 39 events. The GGD shows the lowest scores with respect to the other distributions.**

KS	Means	GGD	Logistic	t-Location	alpha-Stable
delta	Non-Seizure	0.002	0.007	0.007	0.007
	Seizure	0.002	0.004	0.004	0.004
theta	Non-Seizure	0.008	0.037	0.042	0.042
	Seizure	0.005	0.018	0.021	0.021
alpha	Non-Seizure	0.005	0.045	0.051	0.051
	Seizure	0.003	0.021	0.024	0.024
beta	Non-Seizure	0.002	0.024	0.027	0.027
	Seizure	0.001	0.011	0.012	0.012
gamma	Non-Seizure	0.003	0.022	0.027	0.027
	Seizure	0.001	0.010	0.012	0.012
CvM	Means	GGD	Logistic	t-Location	alpha-Stable
delta	Non-Seizure	< 0.001	< 0.001	< 0.001	< 0.001
	Seizure	0.004	0.007	0.006	0.006
theta	Non-Seizure	< 0.001	0.013	0.016	0.016
	Seizure	0.001	0.006	0.008	0.008
alpha	Non-Seizure	< 0.001	0.021	0.027	0.027
	Seizure	< 0.001	0.005	0.006	0.006
beta	Non-Seizure	< 0.001	0.009	0.012	0.012
	Seizure	0.001	0.005	0.006	0.006
gamma	Non-Seizure	< 0.001	0.01	0.016	0.016
	Seizure	< 0.001	0.002	0.003	0.003

**Table 6 – Standard deviations of the KS and CvM scores obtained for GGD pdfs estimated with all EEG segments of the 39 events. The GGD shows the lowest scores with respect to the other distributions.**

KS	St. deviations	GGD	Logistic	t-Location	alpha-Stable
delta	Non-Seizure	0.001	< 0.001	< 0.001	< 0.001
	Seizure	0.024	0.032	0.031	0.031
theta	Non-Seizure	< 0.001	0.002	0.002	0.002
	Seizure	0.014	0.022	0.023	0.023
alpha	Non-Seizure	< 0.001	0.005	0.005	0.005
	Seizure	0.008	0.007	0.007	0.007
beta	Non-Seizure	< 0.001	0.004	0.004	0.004
	Seizure	0.008	0.014	0.016	0.016
gamma	Non-Seizure	0.001	0.004	0.005	0.005
	Seizure	0.002	0.003	0.003	0.003
CvM	St. deviations	GGD	Logistic	t-Location	alpha-Stable
delta	Non-Seizure	0.001	< 0.001	< 0.001	<< 0.001
	Seizure	0.178	0.29	0.258	0.258
theta	Non-Seizure	0.001	0.004	0.003	0.003
	Seizure	0.013	0.064	0.078	0.078
alpha	Non-Seizure	< 0.001	0.007	0.008	0.008
	Seizure	0.005	0.016	0.015	0.015
beta	Non-Seizure	< 0.001	0.006	0.007	0.007
	Seizure	0.028	0.145	0.174	0.174
gamma	Non-Seizure	< 0.001	0.007	0.011	0.011
	Seizure	0.001	0.004	0.005	0.005

their ability to separate such signals, in each brain rhythm. We consider a dataset composed of  $n_1$  non-seizure EEG segments and  $n_2$  seizure segments.

Let  $(\sigma_j^{(N)}, \tau_j^{(N)}) = (\{\sigma_{1j}^{(N)}, \dots, \sigma_{n_1j}^{(N)}\}, \{\tau_{1j}^{(N)}, \dots, \tau_{n_1j}^{(N)}\})$  denote the set of parameters estimated from non-seizure segments for a given rhythm  $j$ . Similarly,  $(\sigma_j^{(S)}, \tau_j^{(S)}) = (\{\sigma_{1j}^{(S)}, \dots, \sigma_{n_2j}^{(S)}\}, \{\tau_{1j}^{(S)}, \dots, \tau_{n_2j}^{(S)}\})$  are the scale and shape parameters of the GGD distributions associated with the wavelet coefficients from seizure segments. It is assumed that these four parameters are independent and follow normal distributions

$$\sigma_j^{(N)} \sim N(\mu_{\sigma_j}^{(N)}, \sigma_{\sigma_j}^{(N)}) \quad (2)$$

$$\sigma_j^{(S)} \sim N(\mu_{\sigma_j}^{(S)}, \sigma_{\sigma_j}^{(S)}) \quad (3)$$

$$\tau_j^{(N)} \sim N(\mu_{\tau_j}^{(N)}, \sigma_{\tau_j}^{(N)}) \quad (4)$$

$$\tau_j^{(S)} \sim N(\mu_{\tau_j}^{(S)}, \sigma_{\tau_j}^{(S)}). \quad (5)$$

A univariate T-test was designed to compare the means  $\mu_{\sigma}^{(N)}$  and  $\mu_{\sigma}^{(S)}$

$$H_0^{(\sigma_j)} : \mu_{\sigma_j}^{(N)} = \mu_{\sigma_j}^{(S)} \quad (6)$$

$$H_1^{(\sigma_j)} : \mu_{\sigma_j}^{(N)} \neq \mu_{\sigma_j}^{(S)}. \quad (7)$$

The variances of the distributions (2)–(5) are not equal and not unknown. Consequently, we designed the test as follows. Let  $\bar{\sigma}_j^{(N)}$  and  $\bar{\sigma}_j^{(S)}$  denote the empirical conditional means of  $\sigma_j^{(N)}$

and  $\sigma_j^{(S)}$ , and  $D_{\sigma_j} = \bar{\sigma}_j^{(N)} - \bar{\sigma}_j^{(S)}$  their difference. Denoting as  $s_{\sigma_j^{(N)}}^2$  and  $s_{\sigma_j^{(S)}}^2$  the unbiased estimators of the variances in each group of segments (i.e. seizure and non-seizure), the standard deviation of  $D_{\sigma_j}$  can be estimated as:

$$\hat{\sigma}_{\sigma_j} = \sqrt{\frac{s_{\sigma_j^{(N)}}^2}{n_1} + \frac{s_{\sigma_j^{(S)}}^2}{n_2}}. \quad (8)$$

The statistics of the T-test associated with (6) and (7) is then

$$T_v^{(\sigma_j)} = \frac{\bar{\sigma}_j^{(N)} - \bar{\sigma}_j^{(S)}}{\sqrt{\frac{s_{\sigma_j^{(N)}}^2}{n_1} + \frac{s_{\sigma_j^{(S)}}^2}{n_2}}}, \quad (9)$$

which is distributed according to a Student's t-distribution with  $\nu$  degrees of freedom,

$$\nu = \frac{\left(\frac{s_{\sigma_j^{(N)}}^2}{n_1} + \frac{s_{\sigma_j^{(S)}}^2}{n_2}\right)^2}{\frac{s_{\sigma_j^{(N)}}^4}{n_1^2(n_1-1)} + \frac{s_{\sigma_j^{(S)}}^4}{n_2^2(n_2-1)}}. \quad (10)$$

The hypothesis  $H_0^{(\sigma_j)}$  is rejected if  $|T_v^{(\sigma_j)}| > T_t$ . In this study, we chose a probability of false alarm  $t = 0.05$ . To assess the statis-

**Table 7 – Decision rules to assess the statistical significance of the difference of means of the GGD parameters for seizure and non-seizure signals.**

p-Value	Observed difference
>0.10	not significant
≤0.10	marginally significant
≤0.05	significant
≤0.01	highly significant

**Table 8 – Results of the t-tests to assess the ability of  $\sigma$  and  $\tau$  to discriminate separately seizure and non-seizure EEG segments. The  $H_0^\sigma$  hypothesis is rejected for all rhythms, with highly statistical significant ( $p < 0.01$ ). These scores are supported by very high Bayes factors. Contrarily,  $H_0^\tau$  is accepted for all rhythms, except Delta. The associated p-values are largely greater than 0.1 with Bayes factors lower than the evidence threshold. We conclude that the scale parameter  $\sigma$  is a marker to discriminate seizure and non-seizure with a high statistical significance. The shape parameter  $\tau$  is not a marker to discriminate seizures and non-seizures.**

GGD parameter	Delta Band ( $\delta$ )		Theta Band ( $\theta$ )		Alpha Band ( $\alpha$ )		Beta Band ( $\beta$ )		Gamma Band ( $\gamma$ )	
	$\sigma$	$\tau$	$\sigma$	$\tau$	$\sigma$	$\tau$	$\sigma$	$\tau$	$\sigma$	$\tau$
$T_v$	6.15	3.19	5.86	0.17	6.47	0.50	7.08	0.48	6.40	0.91
$T_t$	2.09	2.01	2.09	2.03	2.09	2.01	2.07	2.03	2.08	2.01
$p$	<0.001	<0.001	<0.001	0.90	<0.001	0.62	<0.001	0.63	<0.001	0.37
BF	>1000	98.31	>1000	0.03	>1000	0.30	>1000	0.08	>1000	0.64
BF <sub>t</sub>	3.63	2.12	3.70	2.45	3.79	2.09	3.39	2.46	3.51	2.17

tical significance, the p-value of each test has been calculated. Table 7 shows the decision rules that were applied.

A similar test has also been designed to compare  $\mu_{\tau_j}^{(N)}$  and  $\mu_{\tau_j}^{(S)}$  for each brain rhythm  $j$ . A bi-variate T-test has also been designed for the pair  $(\sigma_j, \tau_j)$ . Its results were not significant, therefore it is not reported here. In addition, to further support the statistical significance given by the p-value, we calculated the Bayes factor indicator following the method proposed by [61]. This method establishes a correspondence between frequentist significance tests, such as the ones designed here, with Bayesian tests. As a result it allows one to equate the size of the classical hypothesis tests with evidence thresholds in Bayesian tests. Following this work (and assuming equal variances), we calculated the Bayes factor (BF) that provides the same evidence as the p-values given by our tests

$$BF = \left( \frac{v + T_v^{(\sigma_j)}}{v + (T_v^{(\sigma_j)} - \sqrt{v\gamma^*})^2} \right)^{(n_1+n_2)/2} \quad (11)$$

where the hypothesis  $H_0$  is rejected when  $t > \sqrt{v\gamma^*}$  with  $\gamma^* = \gamma^{2/(n_1+n_2-1)} - 1$  and  $\gamma = ((T_t^{(\sigma_j)})^2 / v - 1)^{(n_1+n_2)/2}$ .

The total amount of EEG were  $n_1 = 26$  non-seizure segments and  $n_2 = 13$  seizure segments. Table 8 shows the T-scores, and their associated p-values and Bayes factors. The corresponding thresholds are shown. We observe that the t-scores ( $T_v^\sigma$ ) are all greater than the threshold ( $T_t$ ). The corresponding p-values ( $p$ ) are all lower than 0.01. The equivalent Bayes factors (BF) are also all greater than the threshold ( $BF_t$ ). The  $H_0^\sigma$  hypothesis is therefore rejected for all brain rhythms, with highly statistical significance according to the decision rules presented in Table 7. The scale parameter  $\sigma$  is a good marker to distinguish seizure and non-seizure EEG segments. Contrarily, t-scores for  $\tau$  are lower than the threshold, except for the Delta rhythm. The associated p-values are higher than 0.1. The Bayes factors are lower than the thresholds. Consequently,  $H_0^\tau$  hypothesis is accepted implying that  $\tau$  cannot discriminate seizure and non-seizure EEG segments. Based on these results, it becomes credible to classify EEG segments into two classes seizure and non-seizure based on the scale parameter of the GGD associated to their wavelet coefficients in each brain rhythm.

## REFERENCES

- [1] Parker JN, Parker PM. The official patient's sourcebook on seizures and epilepsy. The MIT Press; 2003.
- [2] Smithson WH, Walker MC. ABC of epilepsy. BMJ Books; 2012.
- [3] Fisher RS, Acevedo C, Arzimanoglou A, Bogacz A, Cross JH, Elger CE, et al. Ilae official report: a practical clinical definition of epilepsy. *Epilepsy* 2014;55(4):475–82.
- [4] Viglione S, Ordon V, Risch F. A methodology for detecting ongoing changes in the eeg prior to clinical seizures. 21st Western Institute on Epilepsy; 2011.
- [5] Liss S. Apparatus for monitoring and counteracting excess brain electrical energy to prevent epileptic seizures and the like, US patent No. 3850161.
- [6] Ktonas P, Smith J. Quantification of abnormal eeg spike characteristics. *Comput Biol Med* 1974;4(2):157–63.
- [7] Gotman J, Ives J, Gloor P. Automatic recognition of interictal epileptic activity in prolonged eeg recordings. *Electroencephalogr Clin Neurophysiol* 1979;46(5):510–20.
- [8] Iasemidis LD, Zaveri HP, Sackellares JC, Williams WJ. Linear and nonlinear modeling of ECoG in temporal lobe epilepsy. 25th Annual Rocky Mountain Bioengineering Symposium; 1988.
- [9] Iasemidis LD, Zaveri HP, Sackellares JC, Williams WJ. Nonlinear dynamics of electrocorticographic data. *J Clin Neurophysiol* 2006;5(339).
- [10] Sorensen TL, Olsen UL, Conradsen I, Henriksen J, Kjaer TW, Thomsen CE, et al. Automatic epileptic seizure onset detection using matching pursuit: a case study. 32nd Annual International Conference of the IEEE EMB. 2010. pp. 3277–80.
- [11] Liang S-F, Wang H-C, Chang W-L. Combination of eeg complexity and spectral analysis for epilepsy diagnosis and seizure detection. *EURASIP J Adv Signal Process* 2010; 2010(1):853434.
- [12] Bajaj V, Pachori RB. Classification of seizure and nonseizure eeg signals using empirical mode decomposition. *IEEE Trans Inf Technol BioMed* 2012;16(6):1135–42.
- [13] Nasehi S, Pourghassem H. A novel fast epileptic seizure onset detection algorithm using general tensor discriminant analysis. *J Clin Neurophysiol* 2013;30(4):362–70.
- [14] Shoeb A, Edwards H, Connolly J, Bourgeois B, Treves ST, Gutttag J. Patient-specific seizure onset detection. *Epilepsy Behav* 2004;5:483–98.
- [15] Meng L, Frei MG, Osorio I, Strang G, Nguyen TQ. Gaussian mixture models of ecog signal features for improved detection of epileptic seizures. *Med Eng Phys* 2004;26(5):379–93.

- [16] Chan A, Sun F, Boto E, Wingeier B. Automated seizure onset detection for accurate onset time determination in intracranial eeg. *Clin Neurophysiol* 2008;119(12):2687–96.
- [17] Ocak H. Automatic detection of epileptic seizures in eeg using discrete wavelet transform and approximate entropy. *Expert Syst Appl* 2009;36:2027–36.
- [18] Rabbi AF, Fazel-Rezai R. A fuzzy logic system for seizure onset detection in intracranial eeg. *Comput Intell Neurosci* 2012;2012:705140.
- [19] Direito B, Teixeira C, Ribeiro B, Castelo-Branco M, Sales F, Dourado A. Modeling epileptic brain states using eeg spectral analysis and topographic mapping. *J Neurosci Methods* 2012;210(2):220–9.
- [20] Pachori RB. Discrimination between ictal and seizure-free eeg signals using empirical mode decomposition. *Res Lett Signal Process* 2008. 293056.
- [21] BilasPachori R, Bajaj V. Analysis of normal and epileptic seizure eeg signals using empirical mode decomposition. *Comput Methods Prog Biomed* 2011;104(3):373–81.
- [22] Pachori RB, Patidar S. Epileptic seizure classification in eeg signals using second-order difference plot of intrinsic mode functions. *Comput Methods Prog Biomed* 2014;113(2):494–502.
- [23] Supratak A, Li L, Guo Y. Feature extraction with stacked autoencoders for epileptic seizure detection. *Eng Med Biol Soc (EMBC)* 2014.
- [24] Swami P, Gandhi TK, Panigrahi BK, Tripathi M, Anand S. A novel robust diagnostic model to detect seizures in electroencephalography. *Expert Syst Appl* 2016;56:116–30.
- [25] Bhati D, Pachori RB, Gadre VM. A novel approach for time-frequency localization of scaling functions and design of three-band biorthogonal linear phase wavelet filter banks. *Digit Signal Process* 2017;69:309–22.
- [26] Qaraqe M, Ismail M, Serpedin E. Band-sensitive seizure onset detection via csp-enhanced eeg features. *Epilepsy Behav* 2015;50:77–87.
- [27] Acharya U, Oh SL, Hagiwara Y, Tan J, Adeli H. Deep convolutional neural network for the automated detection and diagnosis of seizure using eeg signals. *Comput Biol Med* 2017;17:1–9.
- [28] Hosseini M, Pompili D, Elisevich K, Soltanian-Zadeh H. Random ensemble learning for eeg classification. *Artif Intell Med* 2018;17(S0933-3657):30201–4.
- [29] Logesparan L, Rodriguez-Villegas E, Casson A. The impact of signal normalization on seizure detection using line length features. *Med Biol Eng Comput* 2015;53(10):929–42.
- [30] Bhattacharyya A, Pachori RB, Upadhyay A, Acharya UR. Tunable-q wavelet transform based multiscale entropy measure for automated classification of epileptic eeg signals. *Appl Sci* 2017;7(4):385.
- [31] Bhattacharyya A, Pachori RB, Acharya UR. Tunable-q wavelet transform based multivariate sub-band entropy with application to focal eeg signal analysis. *Entropy* 2017;19(3):99.
- [32] Sharma RR, Pachori RB. A novel approach to detect epileptic seizures using a combination of tunable-q wavelet transform and fractal dimension. *J Mech Med Biol* 2017;17(17):2017.
- [33] Sharma M, Pachori RB, Acharya UR. A new approach to characterize epileptic seizures using analytic time-frequency flexible wavelet transform and fractal dimension. *Pattern Recogn Lett* 2017;94:172–9.
- [34] Fraley C, Raftery AE. Model-based methods of classification: using the mclust software in chemometrics. *J Stat Plan Inference* 2007;18(6):1–13.
- [35] McNicholas P. Model-based classification using latent gaussian mixture models. *J Stat Plan Inference* 2010;140(5):1175–81.
- [36] Saez A, Serrano C, Acha B. Model-based classification methods of global patterns in dermoscopic images. *IEEE Trans Med Imaging* 2014;33(5):1137–47.
- [37] Luessi M, Babacan S, Molina R, Booth J, Katsaggelos A. Bayesian symmetrical eeg/fmri fusion with spatially adaptive priors. *NeuroImage* 2011;55(1):113–32.
- [38] Cortés J, López A, Molina R, Katsaggelos A. Variational bayesian localization of eeg sources with generalized gaussian priors. *Eur Phys J-Plus (EPJP)* 2012;127(140):12140–9.
- [39] EPILEPSIAE. Epilepsiae epilepsy project; 2018, <http://www.epilepsiae.eu/> [accessed 02.02.18].
- [40] Krishnan B, Vlachos I, Faith A, Mullane S, Williams K, Alexopoulos A, et al. A novel spatiotemporal analysis of peri-ictal spiking to probe the relation of spikes and seizures in epilepsy. *Ann Biomed Eng* 2014;42(8):1606–17.
- [41] Joshi V, Pachori RB, Vijesh A. Classification of ictal and seizure-free eeg signals using fractional linear prediction. *Biomed Signal Process Control* 2014;9:1–5.
- [42] Sharma RR, Pachori RB. Classification of epileptic seizures in eeg signals based on phase space representation of intrinsic mode functions. *Expert Syst Appl* 2015;42(3):1106–17.
- [43] Zheng Y, Zhu J, Qi Y, Zheng X, Zhang J. An automatic patient-specific seizure onset detection method using intracranial electroencephalography. *Neuromodulation* 2015;18(2):79–84.
- [44] Kumar TS, Kanhanga V, Pachori RB. Classification of seizure and seizure-free eeg signals using local binary patterns. *Biomed Signal Process Control* 2015;15:33–40.
- [45] Zhang Y, Zhou W, Yuan S. Multifractal analysis and relevance vector machine-based automatic seizure detection in intracranial eeg. *Int J Neural Syst* 2015;25(6):1550020.
- [46] Wang L, Xue W, Li Y, Luo M, Huang J, Cui W, et al. Automatic epileptic seizure detection in eeg signals using multi-domain feature extraction and nonlinear analysis. *Entropy* 2017;19(222).
- [47] Bhattacharyya A, Pachori RB. A multivariate approach for patient specific eeg seizure detection using empirical wavelet transform. *IEEE Trans Biomed Eng* 2017;64(9):2003–15.
- [48] Bhati D, Sharma M, Pachori RB, Gadre VM. Time-frequency localized three-band biorthogonal wavelet filter bank using semidefinite relaxation and nonlinear least squares with epileptic seizure eeg signal classification. *Digit Signal Process* 2017;62:259–73.
- [49] Tiwari AK, Pachori RB, Kanhangad V, Panigrahi BK. Automated diagnosis of epilepsy using key-points based local binary pattern of eeg signals. *IEEE J Biomed Health Inf* 2017;21(4):888–96.
- [50] Sharma RR, Pachori RB. Time-frequency representation using ievdhm-ht with application to classification of epileptic eeg signals, *IET Science. Meas Technol* 2018;12(01):72–82.
- [51] Mallat S. *A Wavelet Tour of Signal Processing*. Academic Press; 2008.
- [52] Do MN, Vetterli M. Wavelet-based texture retrieval using generalized Gaussian density and Kullback–Leibler distance. *IEEE Trans Image Process* 2002;11(2):146–58.
- [53] Pascal F, Bombrun L, Tournet J-Y, Berthoumieu Y. Parameter estimation for multivariate generalized gaussian distributions. *IEEE Trans Signal Process* 2013;61(23):5960–71.
- [54] Goldberger A, Amaral L, Glass L, Hausdorff J, Ivanov P, Mark R, et al. Physiobank, physiotoolkit, and physionet: components of a new research resource for complex physiologic signals. *Circulation* 2000;101(23):e215–20.
- [55] Bandarabadi M, Rasekhi J, Teixeira CA, Netoff TI, Parhi KK, Dourado A. Early seizure detection using neuronal potential similarity: a generalized low-complexity and robust measure. *Int J Neural Syst* 2015;25(05):1550019.

- [56] Quintero-Rincón A, Pereyra M, D'Giano C, Batatia H, Risk M. A new algorithm for epilepsy seizure onset detection and spread estimation from eeg signals. *J Phys: Conf Ser* 2016;705(1):012032.
- [57] Quintero-Rincón A, Prendes J, Pereyra M, Batatia H, Risk M. Multivariate Bayesian classification of epilepsy eeg signals. *IEEE 12th Image, Video, and Multidimensional Signal Processing Workshop (IVMSP)*. 2016. pp. 1–5.
- [58] Quintero-Rincón A, Pereyra M, D'giano C, Batatia H, Risk M. A visual eeg epilepsy detection method based on a wavelet statistical representation and the Kullback–Leibler divergence. *Int Feder Med Biol Eng (IFMBE) Proc* 2017; 60:13–6.
- [59] Laha RC. *Handbook of methods of Applied Statistics Volume I: Techniques of computation, descriptive methods and statistical inference*. John Wiley and Sons; 1967.
- [60] Anderson T. On the distribution of the two-sample Cramer-von Mises criterion. *Ann Math Stat* 1962;33(3):1148–59.
- [61] Johnson VE. Uniformly most powerful Bayesian test. *Ann Stat* 2013;41:1716–41.